Electronic Supplementary Information

Experimental section

Materials: NF was purchased from Shenzhen Green and Creative Environmental Science and Technology Co. Ltd. The $NiCl_2 \cdot 6H_2O$, terephthalic acid, N,N-Dimethyl formamide (DMF) and Hydrochloric acid (HCl) were purchased from Beijing Chemical Works. $RuCl_3 \cdot 3H_2O$ (≥ 43%)were bought from Sigma-Aldrich Chemical Reagent Co., Ltd. The water used throughout all experiments was purified through a Millipore system. All the reagents and chemicals were used as received without further purification.

Preparation of Ni-MOF/NF: Ni-MOF/NF was prepared as follows. 1 mmol $NiCl_2 \cdot 6H_2O$ (0.237 g) and 1 mmol terephthalic acid (0.166 g) were dissolved in 35 mL DMF under magnetic stirring to form a uniform solution. 2.5 mL ethanol and 2.5 mL distilled water were added slowly to the solution under constant stirring for 30 min. Ni foam was cleaned by sonication in water and ethanol for 10 min, was immersed into the solution. Then, the pre-treated Ni foam (2 × 3 cm) and the above solution were transferred into a 50 mL Teflon-lined stainless-steel autoclave and maintained at 125 °C for 12 h. After cooled to room temperature, the product was washed with distilled water for three times and dried at 60 °C in air.

Synthesis of RuO_2: RuO_2 was prepared as follows. Briefly, 2.61 g of $RuCl_3 \cdot 3H_2O$ and 30.0 mL KOH (1.0 M) were added into 100 mL distilled water and stirred for 45 min at 100 °C. Then the above solution was centrifuged for 10 minutes and filtered. The precipitates were collected and washed with water several times. Finally, the product was dried at 80 °C overnight and then annealed at 300 °C in air atmosphere for 3 h. For a typical synthesis of RuO_2/NF electrode, 50 mg RuO_2 was dispersed in 1 mL ethane/water (v:v = 1:1) solution with sonication for 30 min. Then 22.5 μL catalytic inks were dropped on Ni foam (0.5 × 0.5 cm), and dried at 80 °C for 4 h.

Characterizations: XRD data were obtained from a LabX XRD-6100 X-ray diffractometer with Cu Kα radiation (40 kV, 30 mA) of wavelength 0.154 nm (SHIMADZU, Japan). SEM measurements were recorded on a XL30 ESEM FEG scanning electron microscope at an accelerating voltage of 20 kV. TEM images were acquired on a HITACHI H-8100 electron microscopy (Hitachi, Tokyo, Japan) operated at 200 kV. XPS data were collected on an ESCALABMK II x- ray photoelectron spectrometer using Mg as the exciting source. FTIR spectrum was taken on a BRUKER-EQUINOX-55 IR spectrophotometer.

Electrochemical measurements: Electrochemical measurements were performed with a CHI 660E electrochemical analyzer (CH Instruments, Inc., Shanghai) in a standard three-electrode system. Ni-MOF/NF was used as the working electrode. Graphite plate, and an Hg/HgO were used as the counter electrode and the reference electrode, respectively. The temperature of solution was kept at 25 °C for all the measurements via the adjustment of air condition and heating support, which ensured the variation of diffusion coefficient below 1%. The potentials reported in this work were calibrated to RHE other than especially explained, using the following equation: E (RHE) = E (Hg/HgO) + (0.098 + 0.059 pH) V.

FE determination: The FE was calculated by comparing the amount of measured O_2 generated by anodal electrolysis with calculated O_2 (assuming 100% FE). GC analysis was carried out on GC–2014C (Shimadzu Co.) with thermal conductivity detector and nitrogen carrier gas. Pressure data during electrolysis were recorded using a CEM DT-8890 Differential Air Pressure Gauge Manometer Data Logger Meter Tester with a sampling interval of 1 point per second.

Tafel: The linear portions of the Tafel plots are fitted to the Tafel equation ($\eta = b \log j + a$, where η denotes the applied overpotential, j the current density, b the Tafel slope, a the intercept relative to the exchange current density j_0).

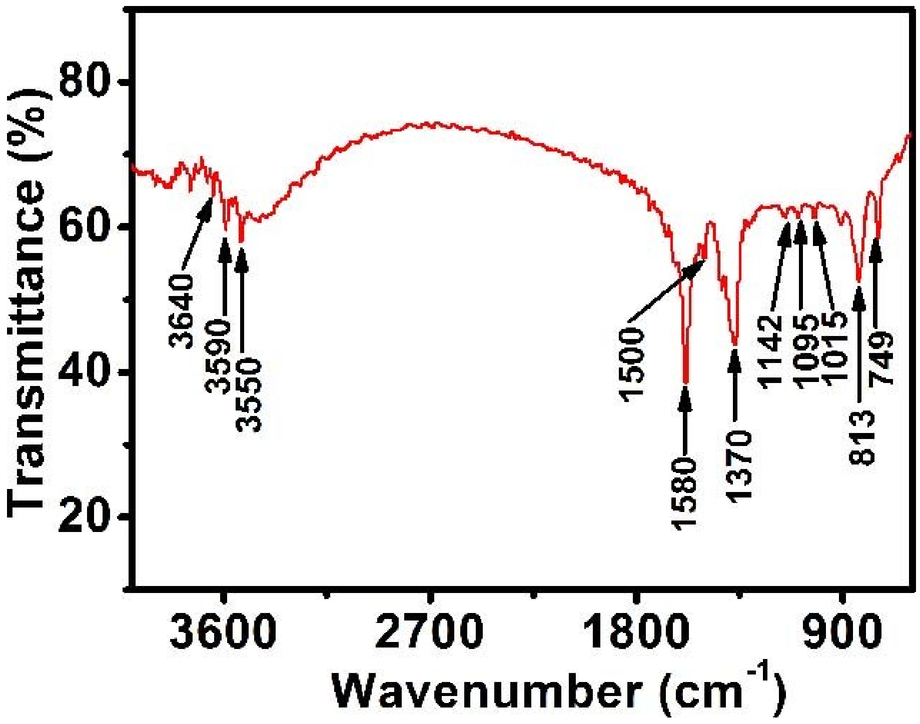

Fig. S1. FT-IR spectrum of Ni-MOF.

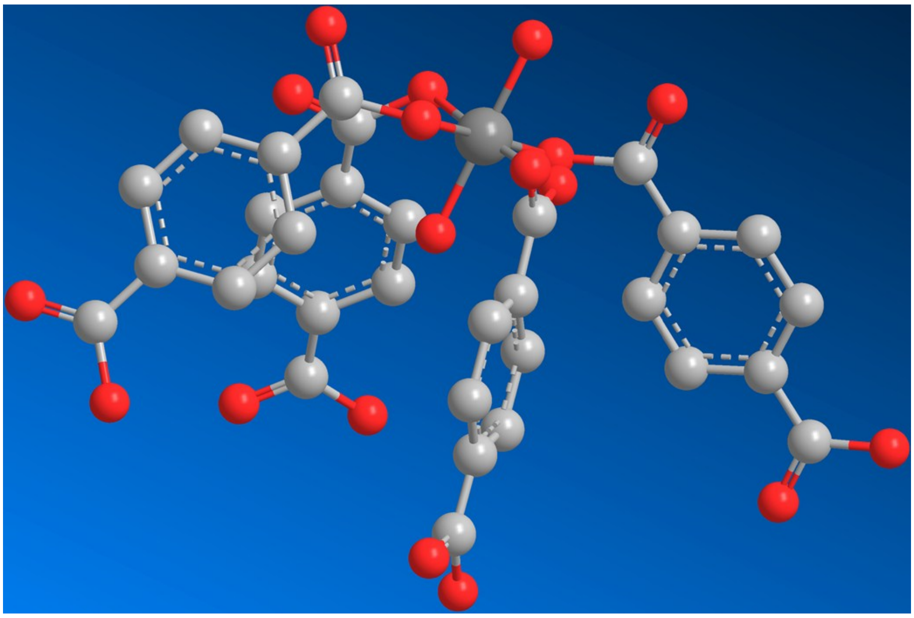

Fig. S2. The structure of Ni-MOF**.**

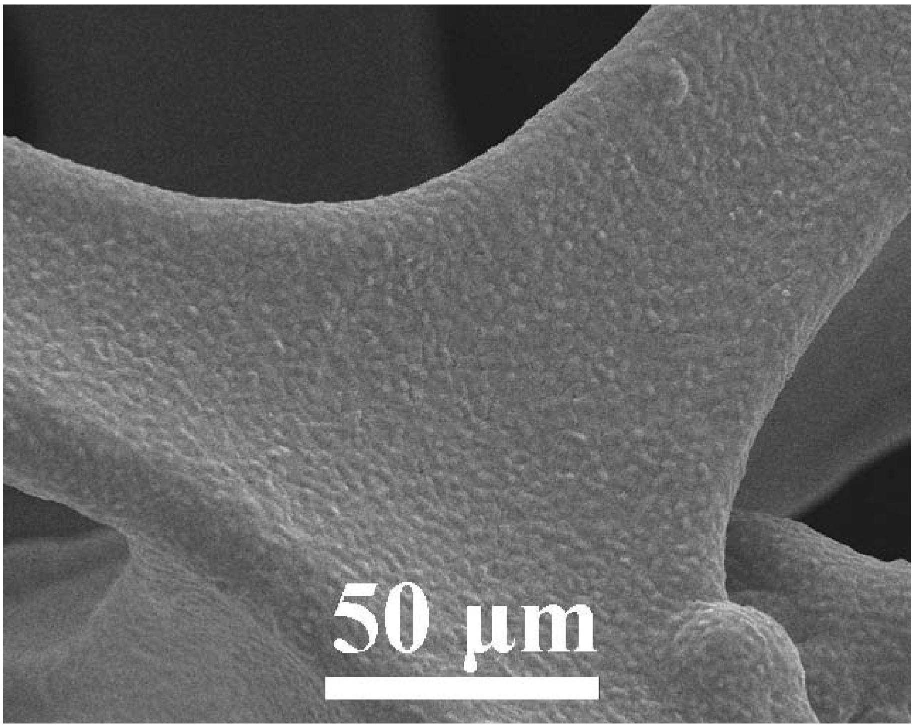

Fig. S3. SEM image of bare NF.

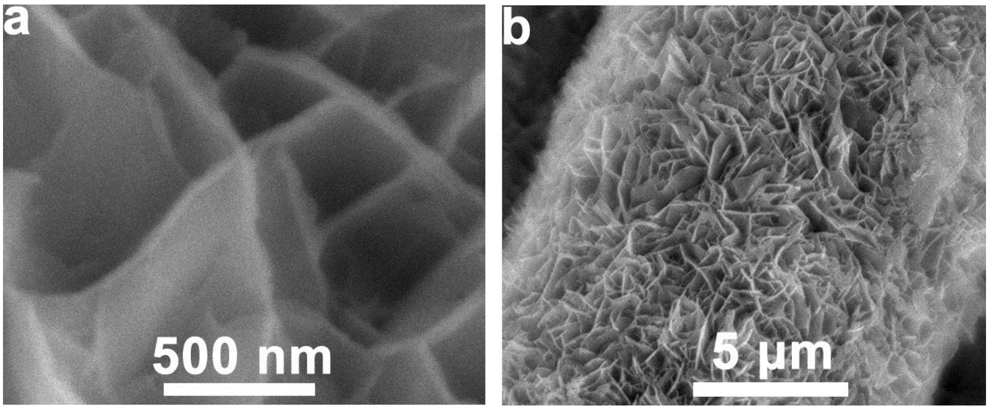

Fig. S4. (a, b) SEM images of Ni-MOF/CC.

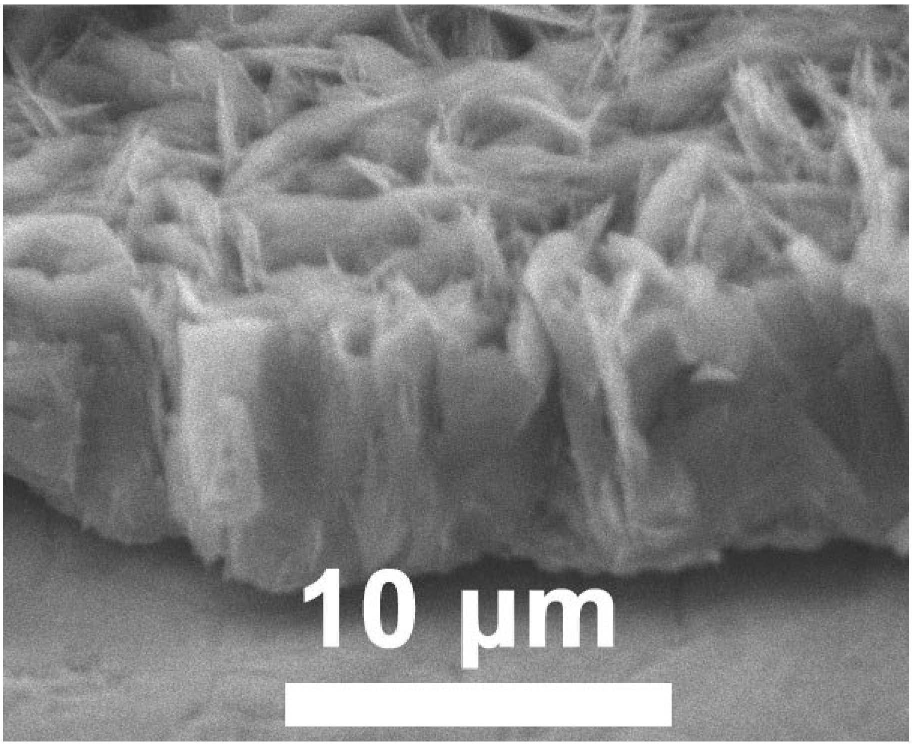

Fig. S5. Cross-section SEM image of Ni-MOF/NF.

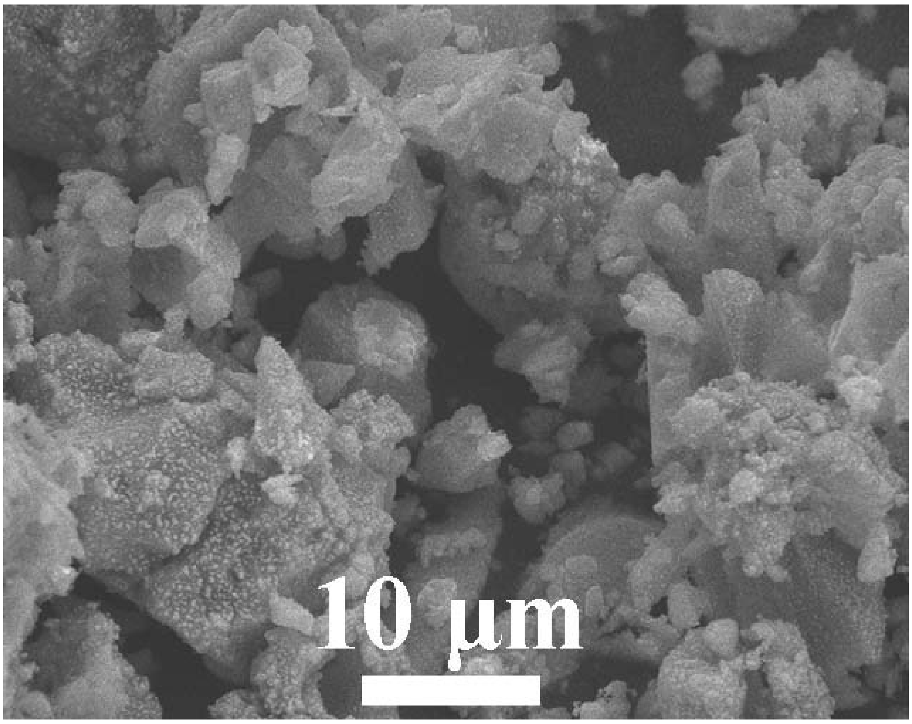

Fig. S6. SEM image of RuO_2 powder.

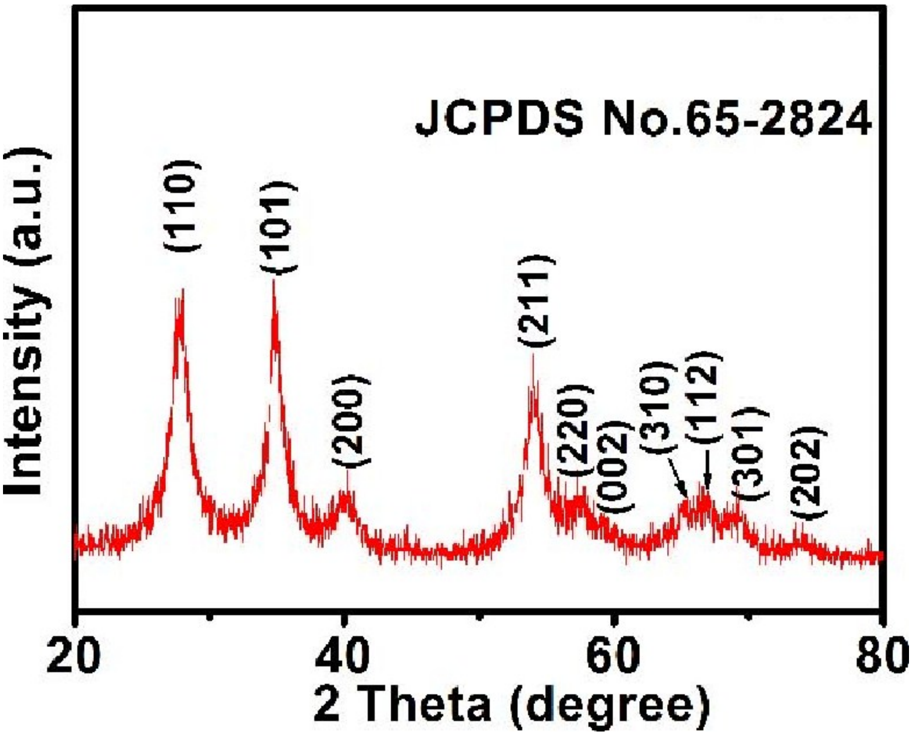

Fig. S7. XRD pattern of RuO_2 powder.

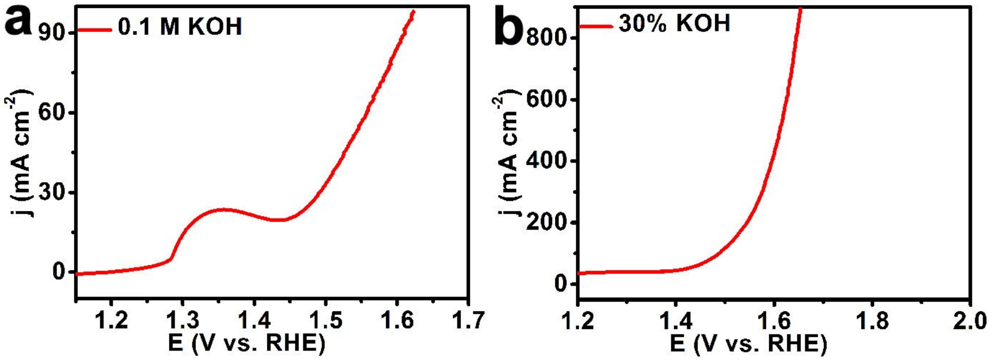

Fig. S8 (a) and (b) LSV curves of Ni-MOF in 0.1 M KOH and 1.0 M KOH, respectively.

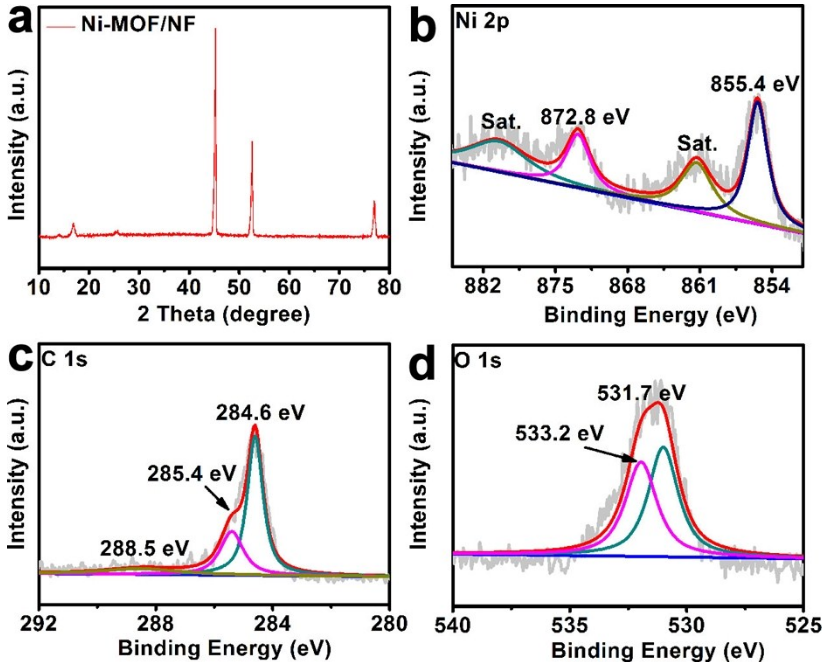

Fig. S9 (a) XRD pattern of Ni-MOF/NF after OER electrolysis. XPS spectra of Ni-MOF after OER electrolysis in the (b) Ni 2p, (c) C 1s, and (c) O 1s regions.

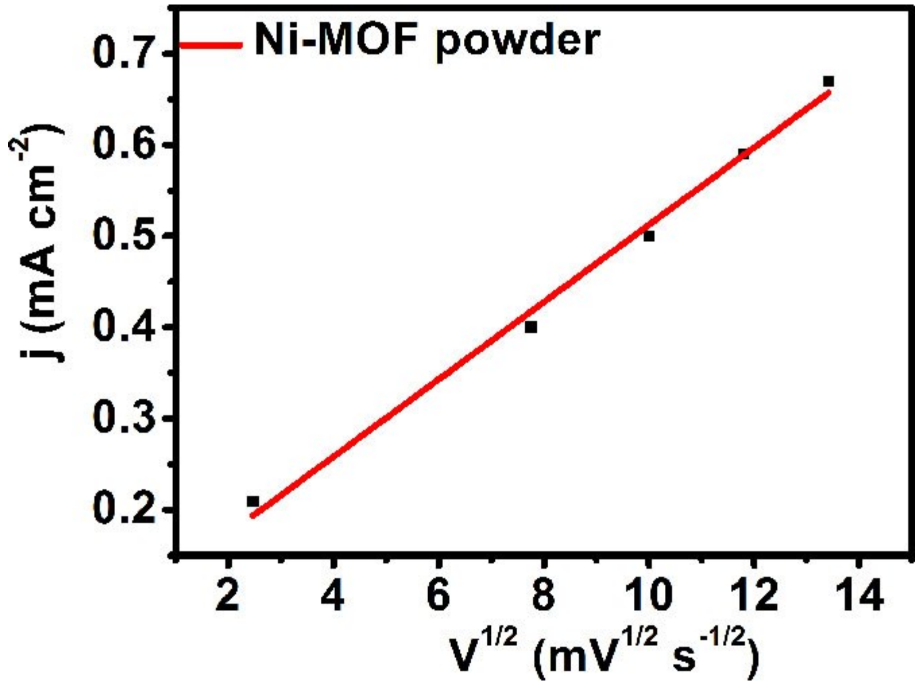

Fig. S10 The relationship between the peak current and the seep rate of the two Ni-MOF electrodes (the currents of the anode was abbreviated as *I*a).

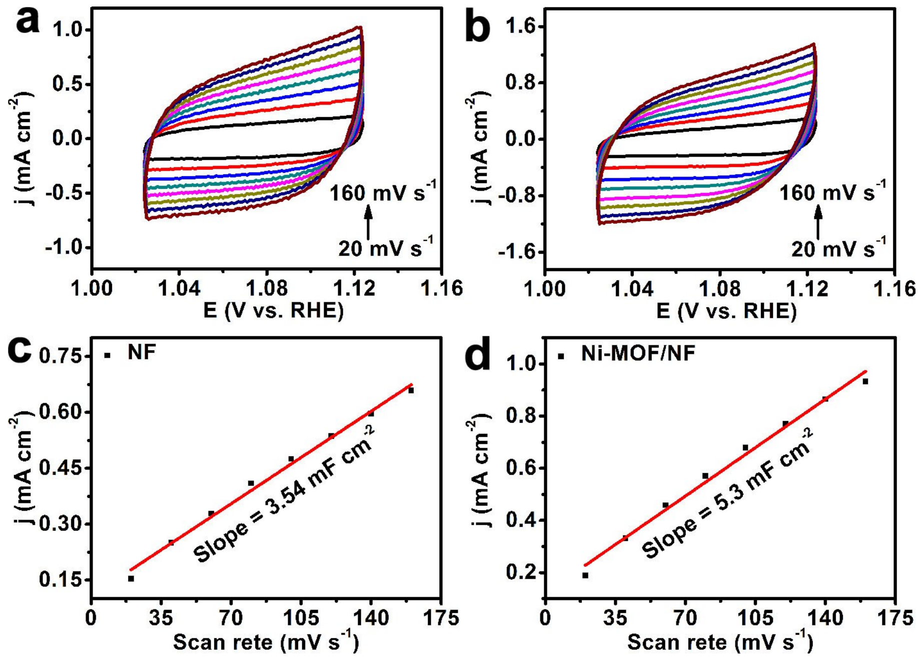

Fig. S11. (a) NF and (b) Ni-MOF/NF in the non-faradaic capacitance current range at scan rates of 20, 40, 60, 80, 100, 120 140 and 160 mV s^{-1}. (c) and (d) the capacitive currents at 1.074 V as a function of scan rate for NF and Ni-MOF/NF.

Table S1. Comparison of OER performance for Ni-MOF/NF with other non-noble-metal electrocatalysts in alkaline media.

Catalyst	**j (mA cm^{-2})**	**η (mV)**	**Electrolyte**	**Ref.**
Ni-MOF	100	320	1.0 M KOH	This work
ALD NiS_X	10	372	1.0 M KOH	1
NiS/Ni foam	100	350	1.0 M KOH	2
NiFe LDH/NF	100	390	1.0 M KOH	3
Ni-P/Ni	100	374	1.0 M KOH	4
Ni_3Se_2/Cu foam	100	388	1.0 M KOH	5
$NiCo_2O_4$	100	430	1.0 M KOH	6
$Ni_{2.3\%}$-CoS_2/C	100	370	1.0 M KOH	7
$NiCo_2S_4$ NA/CC	100	340	1.0 M KOH	8
Ni/Ni3N	100	470	1.0 M KOH	9
CoNi SUNOE	10	450	1.0 M KOH	10
NiFe SUNOE	10	550	1.0 M KOH	10
NiCo LDH	10	367	1.0 M KOH	11
Fe-Ni oxide	10	>375	1.0 M KOH	12
$NiCo_2O_4$ NNs/FTO	10	565	1.0 M KOH	13
β-$Ni(OH)_2$	10	444	1.0 M KOH	14
NiOOH	10	525	1.0 M KOH	15
NiO	10	>470	1.0 M KOH	16
Ni-Co-S/CF	100	363	1.0 M KOH	17
TiN@Ni_3N	10	350	1.0 M KOH	18

References

1 H. Li, Y. Shao, Y. Su, Y. Gao and X. Wang, *Chem. Mater.*, 2016, **28**, 1155–1164.

2 W. Zhu, X. Yue, W. Zhang, S. Yu, Y. Zhang, J Wang and J. Wang, *Chem. Commun.,* 2016, **52**, 1486–1489.

3 J. Luo, J. H. Im, M. T. Mayer, M. Schreier, M. K. Nazeeruddin, N. G. Park, S. D. Tilley, H. J. Fan and M. Grätzel, *Science*, 2014, **345**, 1593–1596.

4 C. Tang, A. M. Asiri, Y. Luo and X. Sun, *ChemNanoMat.*, 2015, **1**, 558–561.

5 J. Shi, J. Hu, Y. Luo, X. Sun and A. M. Asiri, *Catal. Sci. Technol.*, 2015, **5**, 4954–4958.

6 Z. Peng, D. Jia, A. M. Al-Enizi, A. A. Elzatahry and G. Zheng, *Adv. Energy Mater.*, 2015, **5**, 1402031.

7 W. Fang, D. Liu, Q. Lu, X. Sun and A. M. Asiri, *Electrochem. Commun.*, 2016, **63**, 60–64.

8 D. Liu, Q. Lu, Y. Luo, X. Sun and A. M. Asiri, *Nanoscale*, 2015, **7**, 15122–15126.

9 M. Shalom, D. Ressing, X. Yang, G. Clavel, T. P. Fellinger and M. Antonietti, *J. Mater. Chem. A,* 2015, **3**, 8171–8177.

10 B. Ni and X. Wang, *Chem. Sci.*, 2015, **6**, 3572–3576.

11 H. Liang, F. Meng, M. Cabán-Acevedo, L. Li, A. Forticaux, L. Xiu, Z. Wang and S. Jin, *Nano Lett.*, 2015, **15**, 1421–1427.

12 J. Landon, E. Demeter, N. İnoğlu, C. Keturakis, I. E. Wachs, R. Vasić, A. I. Frenkel and J. R. Kitchin, *ACS Catal.*, 2012, **2**, 1793–1801.

13 H. Shi and G. Zhao, *J. Phys. Chem. C*, 2014, **118**, 25939–25946.

14 M. Gao, W. Sheng, Z. Zhuang, Q. Fang, S. Gu, J. Jiang and Y. Yan, *J. Am. Chem. Soc.,* 2014, **136,** 7077–7084.

15 S. Klaus, Y. Cai, M. W. Louie, L. Trotochaud and A. T. Bell, *J. Phys. Chem. C*, 2015, **119,** 7243–7254.

16 L. Kuai, J. Geng, C. Chen, E. Kan, Y. Liu, Q. Wang and B. Geng, *Angew. Chem., Int. Ed*., 2014, **126**, 7677–7681.

17 T. Liu, X. Sun, A. M. Asiri and Y. He, *Int. J. Hydrogen Energy*, 2016, **41**, 7264–7269.

18 Q. Zhang, Y. Wang, Y. Wang, A. M. Al-Enizi, A. A. Elzatahry and G. Zheng, *J. Mater. Chem. A,* 2016, **4**, 5713–5718.